KINETICS OF LASER PLASMA FORMATION IN METAL VAPOUR

V. I. Mazhukin, I. V. Gusew
Institute of Mathematical Modeling, Russian Academy of Science
Miusskaya square 4, 125047 Moscow, Russia

I. Smurov
Ecole Nationale d'Ingénieurs de Saint - Etienne
58 rue Jean Parot, 42023 Saint - Etienne Cédex 2, France

G. Flamant
Institut de Science et de Génie des Matériaux et Procédés, C.N R.S.
B.P.n°5, 66125 Font - Romeu Cédex, France

Abstract

The break–down of metal vapour (Al, Cu) is simulated near the break–down threshold values of laser radiation. The approximation of collision – radiation model are used, including the detail kinetics of excited states with radiation and collision transitions, step–by–step ionization process, unexcitation and recombination. Energy balance is based on two–temperature approximation: for electrons and for heavy particles. It is shown that the particles concentration in excited states and plasma species composition differ rather than Saha – Boltzmann's distribution. Strong dependence of the break–down threshold intensity on initial temperature of neutral and charged particles is shown.

1. Introduction

Optical break–down of evaporated matter near the irradiated surface of a solid consists of a great number of different combined physicochemical phenomena, as a result the gas phase properties change qualitatively. It is transformed from a partially ionized gas transparent for laser radiation into a fully ionized plasma which intensively absorbs laser radiation.

To simulate the kinetics of ionization – recombination processes the collisional – radiational model is used. The comparison of avalanche – like ionization for the vapour of Al and Cu is proposed. These metals have similar parameters of evaporation and ionization potentials close to one another, but their electrons shells are rather different.

2. Physical and Mathematical Model

It is assumed that the metal vapour passing through the Knudsen's layer are initially in the equilibrium state, i.e. initial concentration of atoms and ions in the ground and in the excited states are determined by the Saha – Boltzmann's equations.

The main elementary processes taken into account by the collisional – radiational model are as follows:

1. Spontaneous radiative decay of excited states

   $$A_n^z \xrightarrow{a_{mn}^z} A_m^z + \hbar\omega$$

   where a_{mn}^z (s^{-1}) is radiation transition rate constant, $\hbar\omega$ – released quantum.
2. Excitation and unexcitation of atoms and ions by electron collision

   $$A_n^z + e \overset{k_{mn}^z, k_{nm}^z}{\longleftrightarrow} A_m^z + e$$

   where k_{mn}^z $(cm^3 \cdot s^{-1})$ is electron – particle reaction rate constant for z – charged particle excitation from state m to state n; k_{nm}^z – unexcitation rate constant for the n – th level.
3. Ionization of the ground and excited states of atoms and ions by electron impact

   $$A_n^z + e \xrightarrow{\alpha_n^z} A_0^{z+1} + e + e$$

   where a_{mn}^z $(cm^3 \cdot s^{-1})$ is electron – particle reaction rate constant for the n – th level ionization of z – charged particle.

4. Reaction reversible to the collision ionization: three particles recombination (the third particle is an electron)

$$A_n^z + e + e \xrightarrow{\beta_n^z} A_m^{z-1} + e$$

where β_{mn}^z $(cm^6 \cdot s^{-1})$ is reaction rate constant.

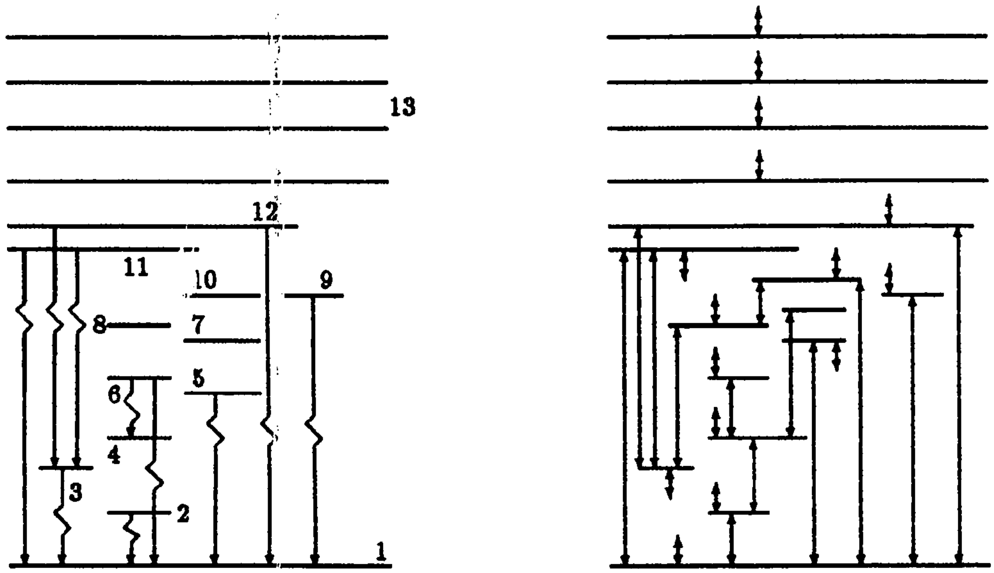

Figure 1: Neutral atom of Al (ionization potential 5.986 eV): scheme of radiation (a) and collision (b) transition; ionization of exited states is indicated by ↕

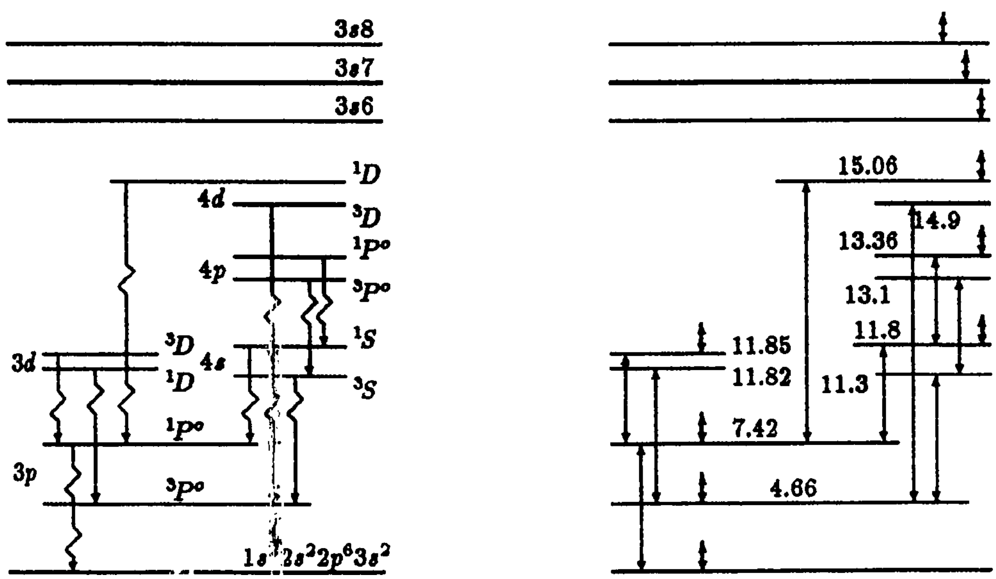

Figure 2: Ion Al+ (ionization potential 18.8237 eV): scheme of radiation (a) and collision (b) transition; ionization of exited states is indicated by ↕

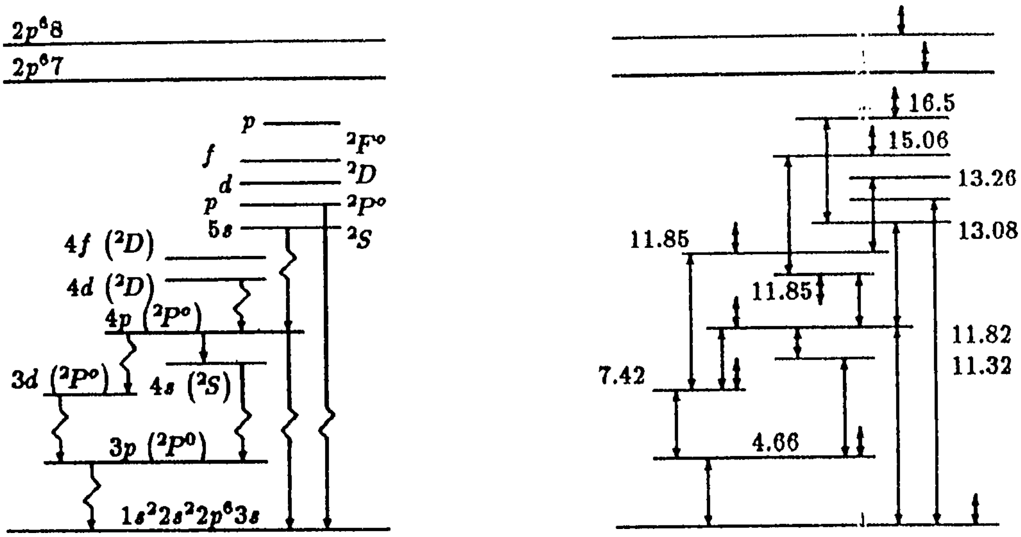

Figure 3: Ion Al^{2+} (ionization potential 28.44 eV): scheme of radiation (a) and collision (b) transition; ionization of exited states is indicated by ↕

Table 1. Energy levels of Al neutral atom Al^{+}, Al^{2+} ions used in the model

№	Al		Al^{1+}		Al^{2+}	
1	$1s^2 2s^2 2p^6 3s^2 3p$	$(^2P^o)$	$1s^2 2s^2 2p^6 3s^2$	(^1S)	$1s^2 2s^2 2p^6 3s$	(^2S)
2	$4s$	(^2S)	$3s3p$	$(^{1,3}P^o)$	$3p$	$(^2P^o)$
3	$3d$	(^2D)	$3s4s$	$(^{1,3}S)$	$3d$	$(^2P^o)$
4	$4p$	$(^2P^o)$	$3s3d$	$(^{1,3})$	$4s$	(^2S)
5	$5s$	(^2S)	$3s4p$	$(^{1,3}P^o)$	$4p$	$(^2P^o)$
6	$4d$	(^2D)	$3s4d$	$(^{1,3}D)$	$4d$	(^2D)
7	$5p$	$(^2P^o)$	$3s6$		$4f$	(^2D)
8	$4f$	$(^2F^o)$	$3s7$		$5s$	(^2S)
9	$6s, p$	$(^2S, ^2P^o)$	$3s8$		$5p$	$(^2P^o)$
10	$5d$	$(^2D^o)$			$5f$	(^2F)
11	$6f$	$(^2F^o)$			$2p^6 7$	
12	$6d, f$	$(^2D, ^2F^o)$			$2p^6 8$	
13	$3s^2 7 - 3s^2 10$				$2p^6 9$	

Charged particles concentration and level-by-level kinetics of neutral atoms and ions is determined by the following system of nonlinear differential equation

$$\frac{dN_i^z}{dt} = N_e \sum_{j \in \Omega_i^z} \left(k_{ji}^z N_j^z - k_{ij}^z N_i^z \right) + N_e \left[\beta_i^z N_e \sum_{j \in \Theta^z} N_j^{z+1} - \alpha_i^z N_i^z \right] - a_i^z N_i^z \qquad (1)$$

$$\frac{dN_e}{dt} = \sum_z \sum_{i \in \Omega_i^z} \left[N_e \sum_{j \in \Omega_i^z} \left(k_{ji}^z N_j^z - k_{ij}^z N_i^z \right) \right], \quad z = 0, 1 \ldots z_{max}, \quad i \in \Theta^z, \qquad (2)$$

where: Θ^z – set of excited states of z – charged particle; Ω_i^z – set of states of z – charged particle, into which collision transition from a state i are taken into account by the model; N_i^z – concentration of z – charged particle in a state i; N_e – density of free electrons; z_{max} – maximal degree of ionization of a neutral atom. It is assumed that for Al vapour $z_{max} = 3$, for Cu vapour $z_{max} = 2$; the excited states of particles having maximal degree of ionization are not taken into account.

Energy balance equations for electrons and heavy particles

$$\frac{d}{dt}\left(\frac{3}{2}N_eT_e\right) = \left\{G\mu - 3\frac{m_e}{M_a}(T_e - Tg)\right\}(\gamma_{en}+\gamma_{ei})N_e + \sum_{s=0}^{s_{max}}\sum_{i\in\Theta^s}\left(Q_i^s+\hat{Q}_i^s\right) \tag{3}$$

$$\frac{3}{2}N_g\frac{d}{dt}(T_g) = 3\frac{m_e}{M_a}(T_e - Tg)(\gamma_{en}+\gamma_{ei})N_e \tag{4}$$

where: ω, γ_{en}, γ_{ei} – frequencies of laser radiation, electron – neutral and electron – ion collisions, respectively; Q_i^s – energy exchange due to excitation and unexcitation of energy level, $\hat{Q}_i^s$ – energy exchange due to ionization and three particles recombination.

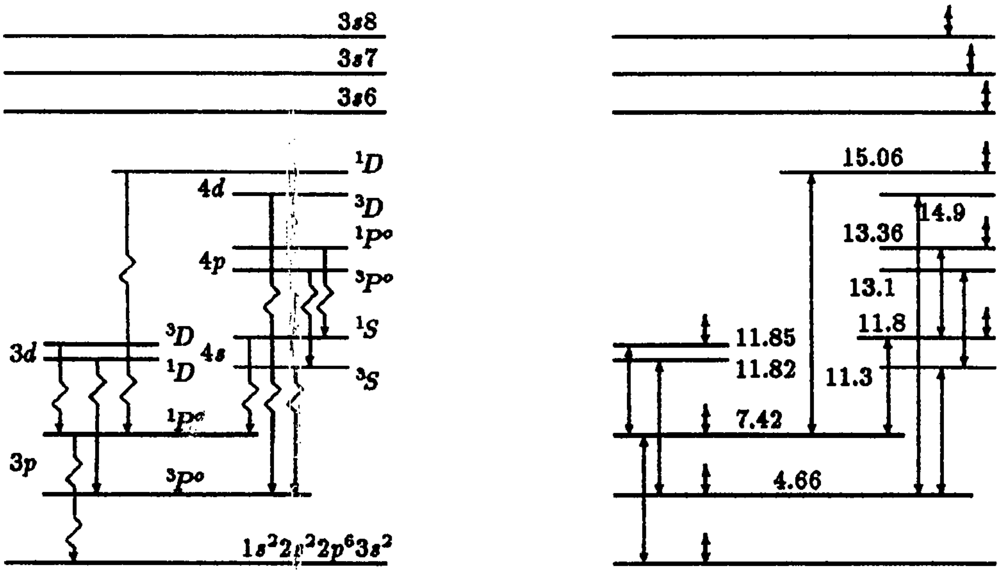

Figure 4: Cu neutral atom (ionization potential 7.762 eV): scheme of radiation (a) and collision (b) transition; ionization of exited states is indicated by ↕

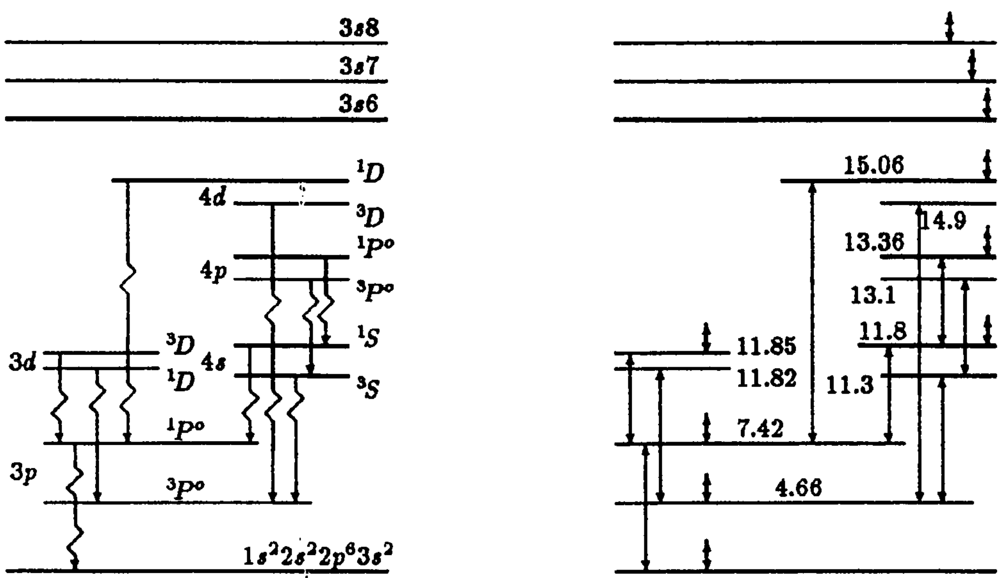

Figure 5: Ion Cu^+ (ionization potential 20.291 eV): scheme of radiation (a) and collision (b) transition; ionization of exited states is indicated by ↕

Table 2. Energy levels of Cu neutral atom and Cu^{+} ion used in the model

Nº	Cu		Cu^{1+}	
1	$3s^2 3p^6 3d^{10} 4s$	$(^2S_{1/2})$	$3s^2 3p^6 3d^{10}$	$(^2S_0)$
2	$4s^2$	(^2D)	$4s$	$(^{1,3}D)$
3	$4p'$	$(^{2,4}P^o, ^2F^o, ^{2,4}D^o)$	$4p$	$(^1P^o, ^{1,3}D^o, ^3F^o,)$
4	$4d$	(^2D)	$5s$	(^3D)
5	$5s$	$(^2S, ^4D)$	$5p$	$(^3D, ^3G, ^3F, ^3F^o, ^3P^o)$
6	$5p$	$(^2P^o)$	$6s$	(^3D)
7	$6p$	$(^2P^o)$	$3d^9 8$	
8	$7p$	$(^2P^o)$	$3d^9 9$	
9	$3d^{10}8 - 3d^{10}10$		$3d^9 10$	

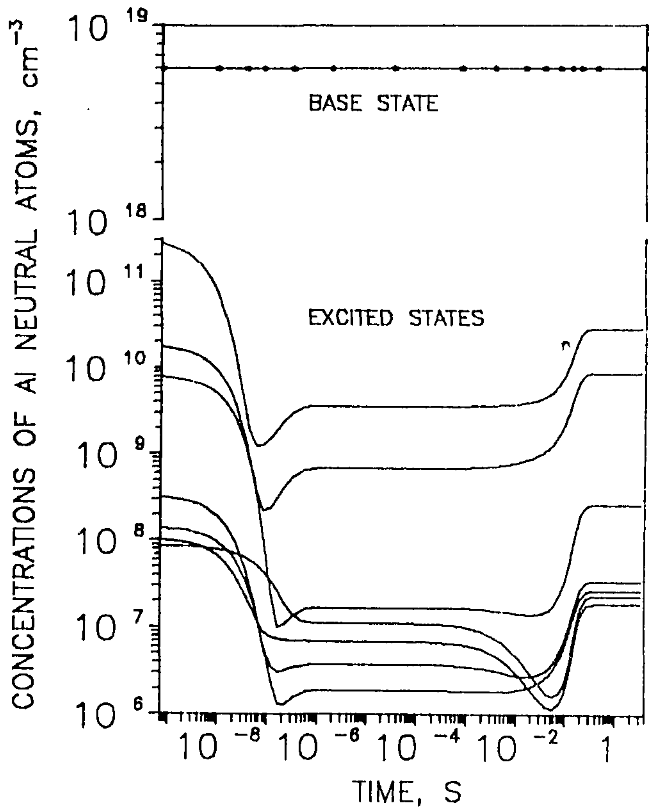

Figure.6 Density of exited states for Al neutral atoms; the order of curves (from up to down) corresponds to the energy levels from Table 1. Intensity of laser radiation $G = 10^7$ W/cm^2, initial density of atoms $N^0_{at} = 6 \cdot 10^{18} cm^{-3}$, initial vapour temperature 0.2 eV.

3. Results and Discussion

The values of laser intensity used in the simulation correspond the near break–down threshold values ($\lambda = 1.06$ $\mu m, G = 10^6 \div 10^9$ W/cm^2 for Al, $G = 10^6 \div 10^{10}$ W/cm^2 for Cu). The initial values of vapour temperature T^0 and density ρ^0 are equal for both metals and correspond to the Knudsen's layer values during intensive evaporation: $T^0 = 0.2$ eV, $\rho^0 = 6 \cdot 10^{18}$ cm^{-3}, $N_e = \sum N_j = 4 \cdot 10^{13}$ cm^{-3}.

The two typical regimes are considered:

(a). laser intensity is below the threshold values of avalanche–like ionization ($G < 10^9$ W/cm^2 for Al, $G < 2 \cdot 10^8$ W/cm^2 for Cu);

(b). optical break–down development when a partially ionized gas transforms into a fully ionized plasma.

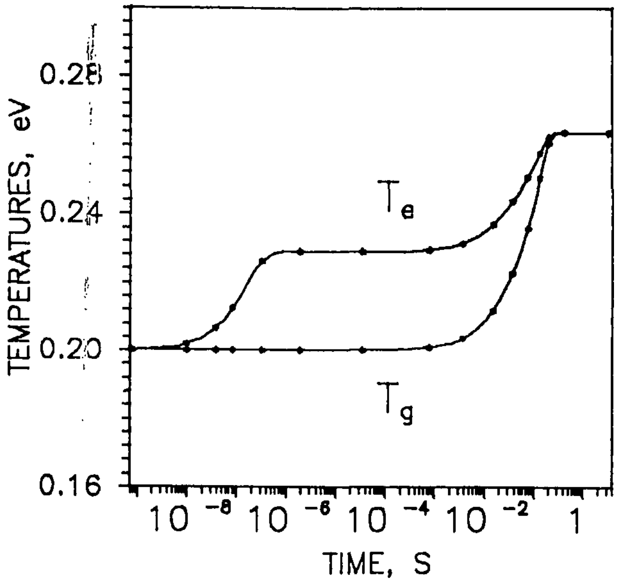

Figure.7 Temperature of electrons T_e and heavy particles (atoms, ions) in Al vapour ($G = 10^7\ W/cm^2$).

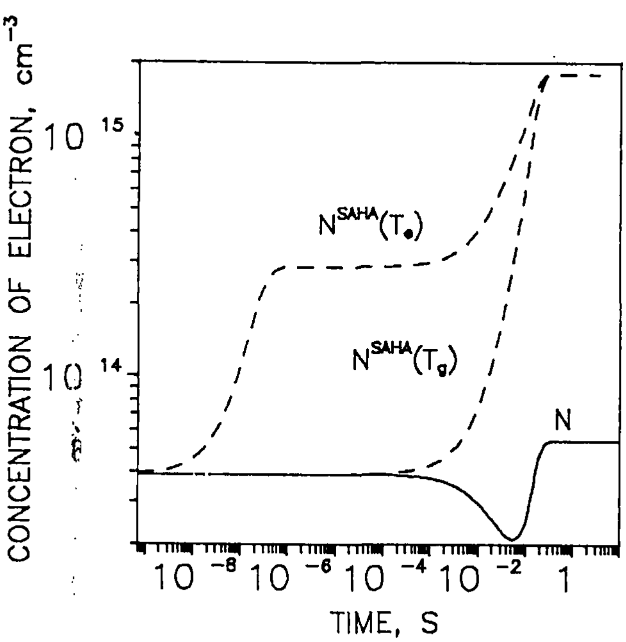

Figure.8 Concentration of charged particles ($N_e \sim N_i$) in Al vapour ($G = 10^7\ W/cm^2$). Dashed curves: equilibrium concentration of charged particles (based on Saha equations) for T_e, T_g temperatures.

(a). When intensi[illegible] laser radiation is below the threshold values (Figures 6 – 11) metal vapour from initial equilibrium state, passing through the transient stage of different nonequilibrium processed, finally reach another stationary equilibrium state, which differ rather from Saha – Boltzmann's distribution.
(b). During optical break-down (Figures 12,13) metal vapour, as a result of nonequilibrium step-by-step ionization, transform into plasma which composition completely coincide with the Saha – Boltzmann's one. The threshold intensities of laser radiation versus initial vapour temperature and duration of laser action are presented in Figures 14.

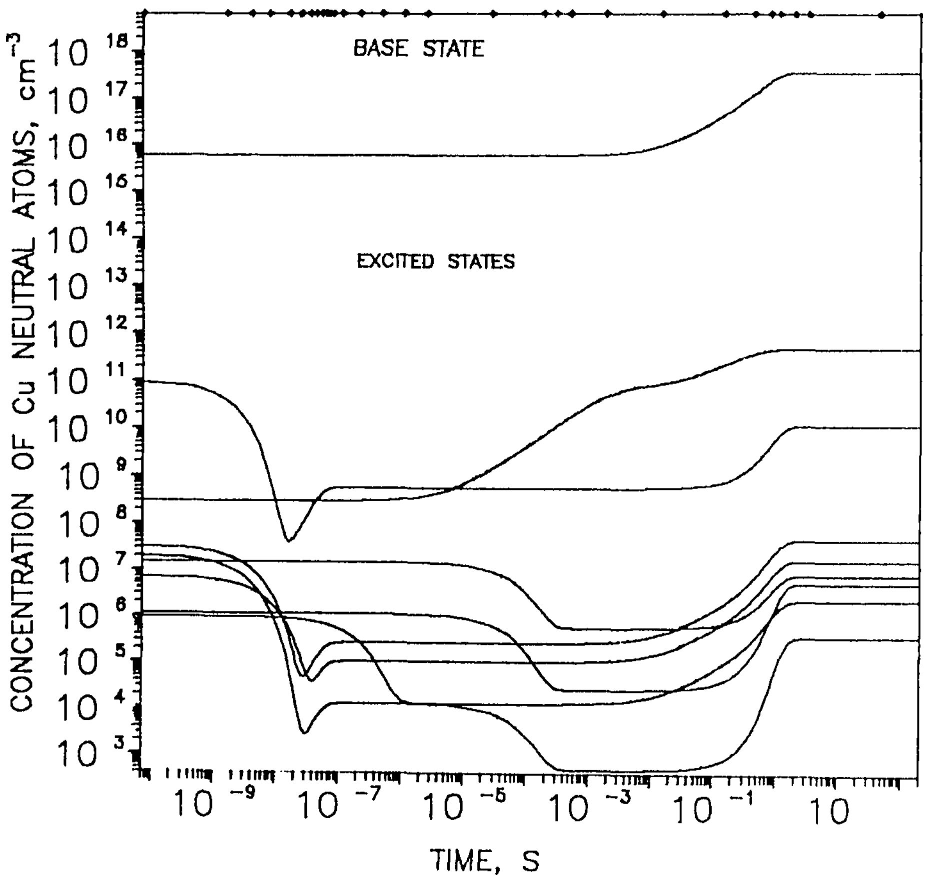

Figure.9 Density of excited states for Cu neutral atoms; the order of curves (from up to down) corresponds to the energy levels from Table 2. Intensity of laser radiation $G = 10^8\ W/cm^2$, initial density of atoms $N^0_{at} = 6 \cdot 10^{18}\ cm^{-3}$, initial vapour temperature 0.2 eV

4. Conclusion

(1). The threshold intensities of laser radiation required for optical break-down of Al and Cu are different about ten times, because of their electron shells difference.
(2). The dynamics of vapour excitation and ionization always include sufficiently nonequilibrium stage that makes impossible to use Saha – Boltzmann's approach to determine plasma species composition and corresponding radiative properties.
(3). The increase of initial temperature of vapour leads to a sharp decrease of the threshold intensities and durations of laser irradiation required for optical break-down.

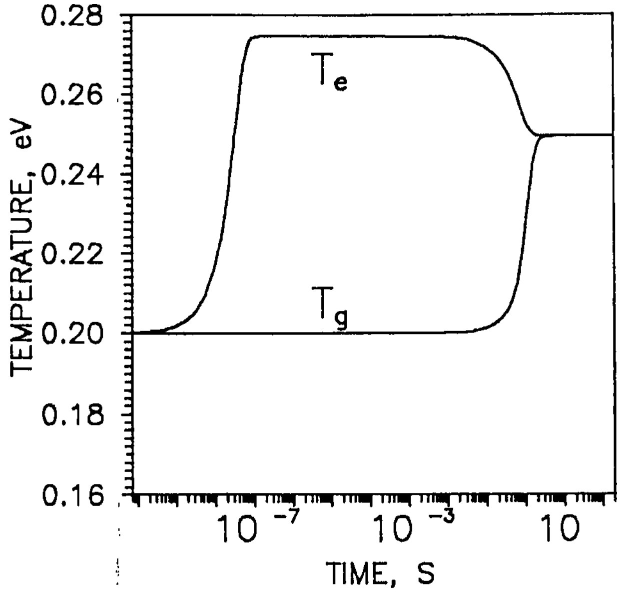

Figure.10 Temperature of electrons T_e and heavy particles (atoms, ions) in Cu vapour ($G = 10^8$ W/cm^2).

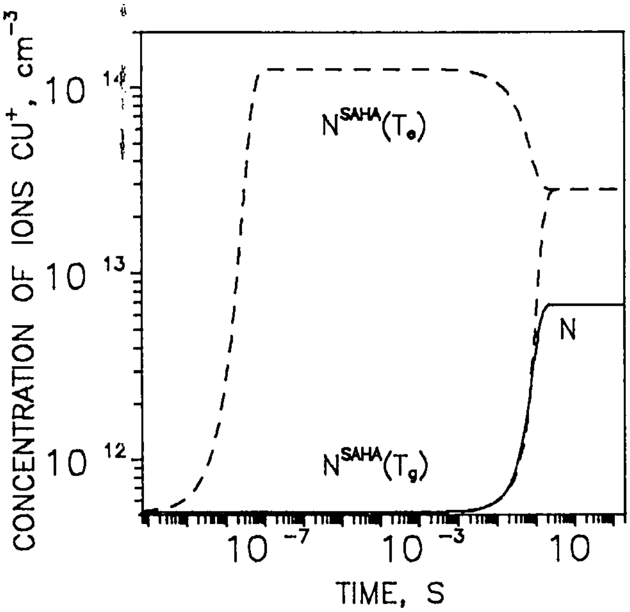

Figure.11 Concentration of charged particles ($N_e \sim N_i$ in Cu vapour ($G = 10^8$ W/cm^2). Dashed curves: equilibrium concentration of charged particles (based on Saha equations) for T_e, T_g temperatures.

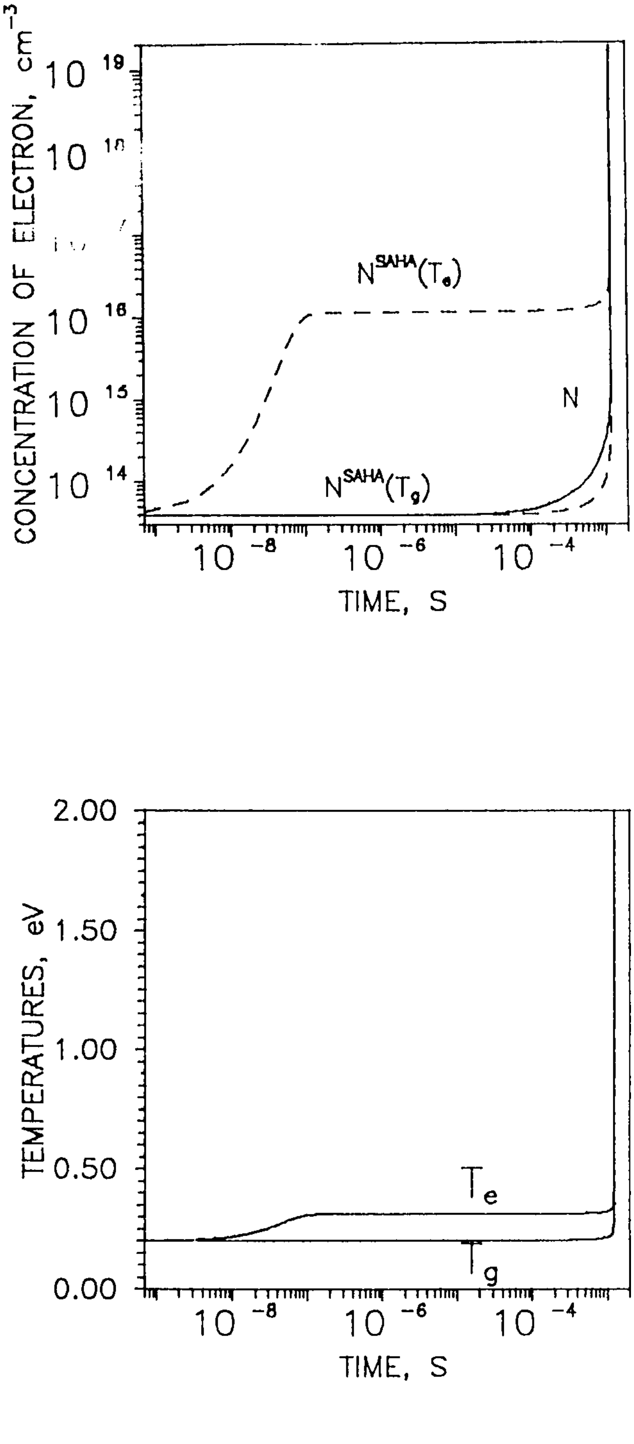

Figure.12 Optical break-down of Al vapour ($G = 10^6\ W/cm^2$, initial density of atoms $N_{at}^0 = 6 \cdot 10^{16} cm^{-3}$, initial vapour temperature 0.2 eV): concentration of charged particles ($N_e \sim \sum N_i$), temperatures of electrons T_e and ions T_g. Dashed curves: equilibrium concentrations of charged particles (based on Saha equations) for T_e, T_g temperatures.

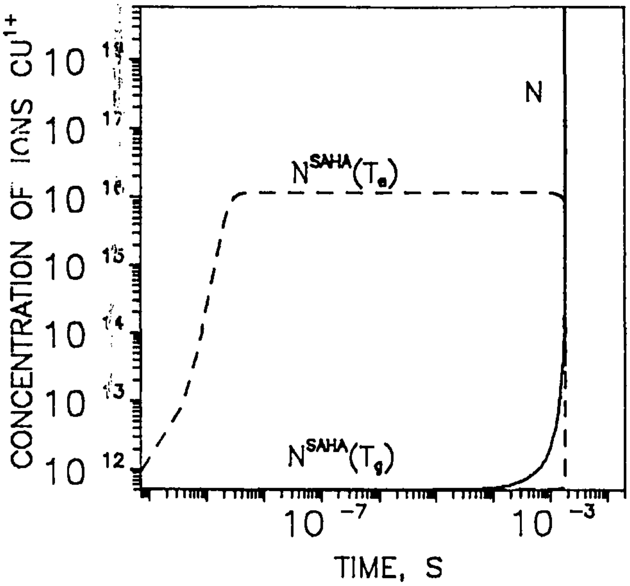

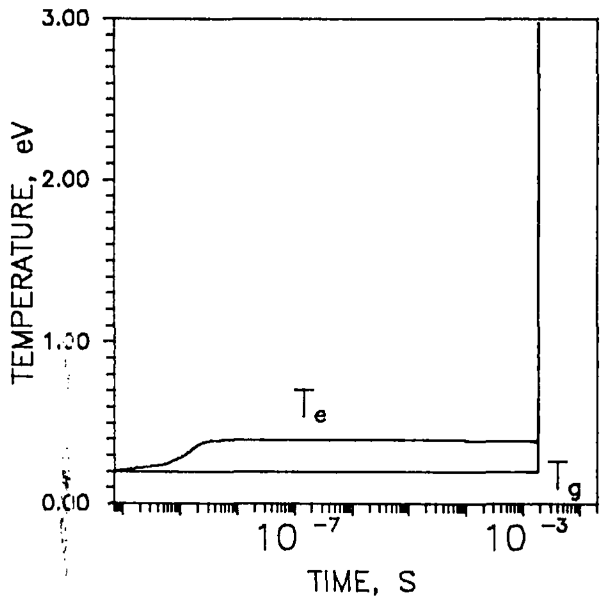

Figure.13 Optical break–down of Cu vapour ($G = 5 \cdot 10^9\ W/cm^2$, initial density of atoms $N_{at}^0 = 6 \cdot 10^{18} cm^{-3}$, initial vapour temperature 0.2 eV): concentration of charged particles ($N_e \sim \sum N_i$), temperatures of electrons T_e and ions T_g. Dashed curves: equilibrium concentrations of charged particles (based on Saha equations) for T_e, T_g temperatures.

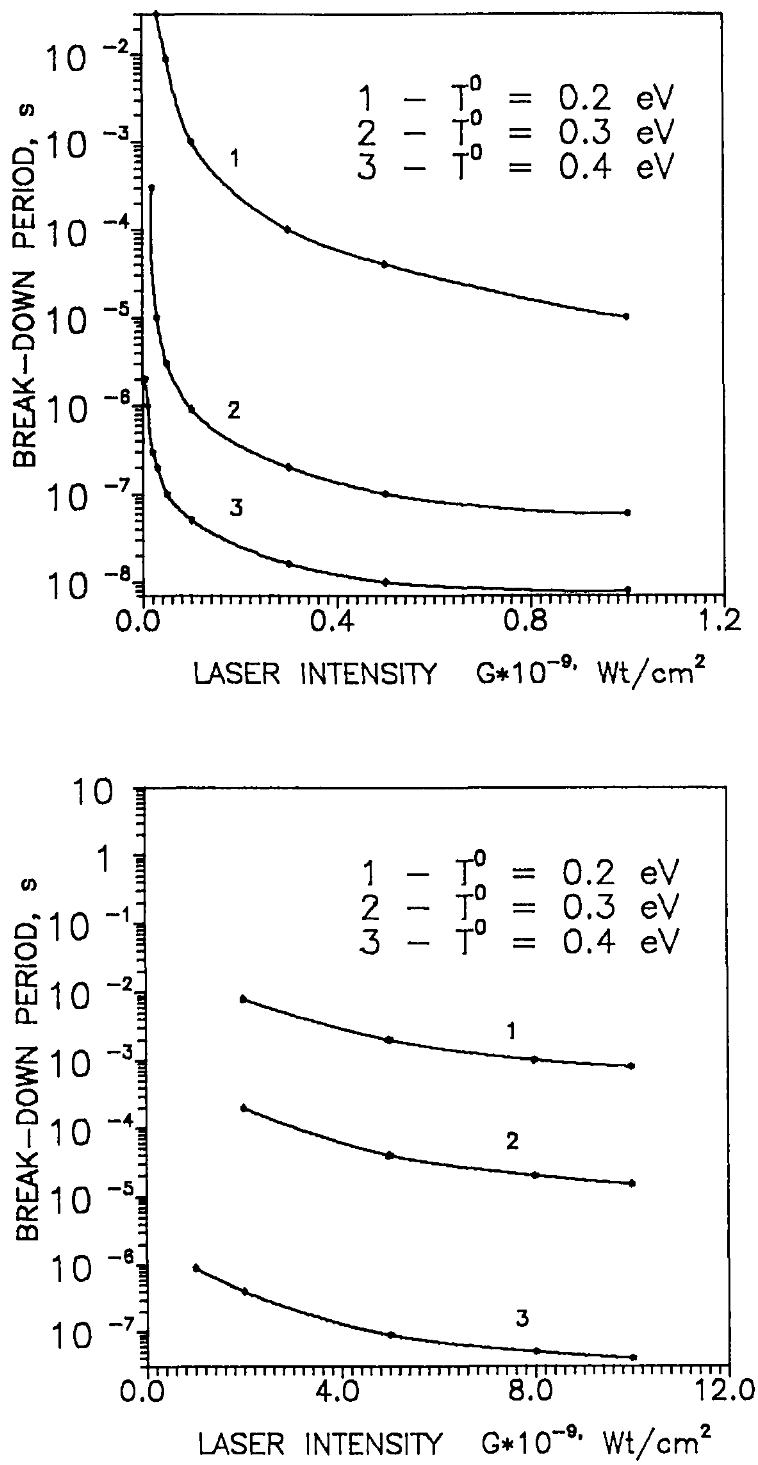

Figure.14 The dependence of break–down period for Al (a) and Cu (b) versus laser radiation intensity G for different values of initial temperature T^0